

Dissipative numerical methods for the Hunter-Saxton equation

Yan Xu* and Chi-Wang Shu[†]

Abstract

In this paper, we present further development of the local discontinuous Galerkin (LDG) method designed in [21] and a new dissipative discontinuous Galerkin (DG) method for the Hunter-Saxton equation. The numerical fluxes for the LDG and DG methods in this paper are based on the upwinding principle. The resulting schemes provide additional energy dissipation and better control of numerical oscillations near derivative singularities. Stability and convergence of the schemes are proved theoretically, and numerical simulation results are provided to compare with the scheme in [21].

AMS subject classification: 65M60, 37K10

Key words: discontinuous Galerkin method, local discontinuous Galerkin method, dissipation, Hunter-Saxton equation, stability

*Department of Mathematics, University of Science and Technology of China, Hefei, Anhui 230026, P.R. China. Email: yxu@ustc.edu.cn. Research supported by NSFC grant 10601055, FANEDD of CAS and SRF for ROCS SEM.

[†]Division of Applied Mathematics, Brown University, Providence, RI 02912, USA. E-mail: shu@dam.brown.edu. Research supported by NSF grant DMS-0809086 and ARO grant W911NF-08-1-0520.

1 Introduction

In this paper, we present further development of the local discontinuous Galerkin (LDG) method designed in [21] and a new dissipative discontinuous Galerkin (DG) method for the Hunter-Saxton (HS) equation

$$u_{xxt} + 2u_x u_{xx} + uu_{xxx} = 0. \tag{1.1}$$

In [21], we developed a LDG method for the HS type equations and gave a rigorous proof for its energy stability. In this method the basis functions used are discontinuous in space. The LDG discretization also results in a high order accurate, extremely local, element based discretization. In particular, the LDG method is well suited for *hp*-adaptation, which consists of local mesh refinement and/or the adjustment of the polynomial order in individual elements. Numerical simulation shows that the LDG method in [21] approximates the dissipative regularization and the dispersive regularization, as well as continuous solutions of the original HS equation (with possibly discontinuous derivatives) quite well. However, when the derivative has a big jump discontinuity, the LDG solution for the derivative contains spurious numerical oscillations, which are controlled by a nonlinear limiter in [21]. In this paper, we attempt to improve the performance of the LDG method in its control on spurious numerical oscillations near derivative singularities, without sacrificing its accuracy and provable stability. We also design a new dissipative DG method with the same improved numerical performance and provable convergence for the piecewise constant case.

The DG method is a class of finite element methods, using discontinuous, piecewise polynomials as the solution and the test space. It was first designed as a method for solving hyperbolic conservation laws containing only first order spatial derivatives, e.g. Reed and Hill [15] for solving linear equations, and Cockburn et al. [4, 3, 2, 6] for solving nonlinear equations. It is difficult to apply the DG method directly to the equations with higher order derivatives. The LDG method is an extension of the DG method aimed at solving partial differential equations (PDEs) containing higher than first order spatial derivatives. The first LDG method was constructed by Cockburn and Shu in [5] for solving nonlinear convection diffusion equations containing second order

spatial derivatives. Their work was motivated by the successful numerical experiments of Bassi and Rebay [1] for the compressible Navier-Stokes equations. The idea of the LDG method is to rewrite the equations with higher order derivatives into a first order system, then apply the DG method on the system. The design of the numerical fluxes is the key ingredient to ensure stability. The LDG techniques have been developed for convection diffusion equations (containing second derivatives) [5], nonlinear one-dimensional and two-dimensional KdV type equations [22, 19] and the Camassa-Holm equation [20]. More general information about DG methods for elliptic, parabolic and hyperbolic partial differential equations can be found in the two special journal issues devoted to the DG method [7, 8], as well as in the recent books and lecture notes [14, 9, 16, 17].

This paper is organized as follows. In Section 2, we present and analyze our improved, dissipative LDG method for the HS type equations (1.1). We give a proof of the energy stability in Section 2.3. In Section 3, we present a new dissipative DG method for the HS equation. Stability for general case is proved, as well as convergence for the piecewise constant P^0 case. Section 4 contains numerical results to compare with the results in [21] and to demonstrate the accuracy and capability of the methods. Concluding remarks are given in Section 5.

2 The dissipative LDG method for the HS equation

2.1 Notation

We denote the mesh in $[0, L]$ by $I_j = [x_{j-\frac{1}{2}}, x_{j+\frac{1}{2}}]$, for $j = 1, \dots, N$. The center of the cell is $x_j = \frac{1}{2}(x_{j-\frac{1}{2}} + x_{j+\frac{1}{2}})$ and the mesh size is denoted by $h_j = x_{j+\frac{1}{2}} - x_{j-\frac{1}{2}}$, with $h = \max_{1 \leq j \leq N} h_j$ being the maximum mesh size. We assume that the mesh is regular, namely that the ratio between the maximum and the minimum mesh sizes stays bounded during mesh refinements. We define the piecewise-polynomial space V_h as the space of polynomials of the degree up to k in each cell I_j , i.e.

$$V_h = \{v \in L^2(\Omega) : v \in P^k(I_j) \text{ for } x \in I_j, \quad j = 1, \dots, N\}.$$

Note that functions in V_h are allowed to have discontinuities across element interfaces.

The solution of the numerical scheme is denoted by u_h , which belongs to the finite element space V_h . We denote by $(u_h)_{j+\frac{1}{2}}^+$ and $(u_h)_{j+\frac{1}{2}}^-$ the values of u_h at $x_{j+\frac{1}{2}}$, from the right cell I_{j+1} , and from the left cell I_j , respectively. We use the usual notations $[u_h] = u_h^+ - u_h^-$ and $\bar{u}_h = \frac{1}{2}(u_h^+ + u_h^-)$ to denote the jump and the mean of the function u_h at each element boundary point, respectively.

2.2 The LDG method

In this section, we define our LDG method for the HS equations (1.1), written in the following form

$$u_{xx} = q, \quad (2.1)$$

$$q_t = \frac{1}{2}((u_x)^2)_x - \frac{1}{2}(u^2)_{xxx} \quad (2.2)$$

with an initial condition

$$u(x, 0) = u_0(x), \quad (2.3)$$

and the boundary conditions

$$u(0, t) = u_x(0, t) = u_x(L, t) = 0, \quad (2.4)$$

or

$$u(L, t) = u_x(0, t) = u_x(L, t) = 0. \quad (2.5)$$

To define the local discontinuous Galerkin method, we further rewrite the equation (2.1) as a first order system:

$$q - r_x = 0, \quad (2.6)$$

$$r - u_x = 0.$$

The LDG method for the equations (2.6), where q is assumed known and we would want to solve for u , is formulated as follows: find $u_h, r_h \in V_h$ such that, for all test functions $\rho, \vartheta \in V_h$,

$$\int_{I_j} q_h \rho dx + \int_{I_j} r_h \rho_x dx - (\widehat{r}_h \rho^-)_{j+\frac{1}{2}} + (\widehat{r}_h \rho^+)_{j-\frac{1}{2}} = 0, \quad (2.7a)$$

$$\int_{I_j} r_h \vartheta dx + \int_{I_j} u_h \vartheta_x dx - (\widehat{u}_h \vartheta^-)_{j+\frac{1}{2}} + (\widehat{u}_h \vartheta^+)_{j-\frac{1}{2}} = 0. \quad (2.7b)$$

The “hat” terms in (2.7) in the cell boundary terms from integration by parts are the so-called “numerical fluxes”, which are single valued functions defined on the edges and should be designed based on different guiding principles for different PDEs to ensure stability. For the standard elliptic equation (2.6), we can take the simple choices such that

$$\widehat{r}_h = r_h^+, \quad \widehat{u}_h = u_h^-, \quad (2.8)$$

where we have omitted the half-integer indices $j+\frac{1}{2}$ as all quantities in (2.8) are computed at the same points (i.e. the interfaces between the cells).

Equation (2.2) can be rewritten as a first order system:

$$\begin{aligned} q_t + p_x - B(r)_x &= 0, \\ p - (b(r)u)_x &= 0, \\ r - u_x &= 0, \end{aligned} \quad (2.9)$$

where $B(r) = \frac{1}{2}r^2$ and $b(r) = B'(r) = r$. Now we can define a local discontinuous Galerkin method to equations (2.9), resulting in the following scheme: find $q_h, p_h, r_h \in V_h$ such that, for all test functions $\varphi, \psi, \eta \in V_h$,

$$\int_{I_j} (q_h)_t \varphi dx - \int_{I_j} (p_h - B(r_h)) \varphi_x dx + ((\widehat{p}_h - \widehat{B(r_h)}) \varphi^-)_{j+\frac{1}{2}} - ((\widehat{p}_h - \widehat{B(r_h)}) \varphi^+)_{j-\frac{1}{2}} = 0, \quad (2.10a)$$

$$\int_{I_j} p_h \psi dx + \int_{I_j} b(r_h) u_h \psi_x dx - (\widehat{b(r_h)} \widetilde{u}_h \psi^-)_{j+\frac{1}{2}} + (\widehat{b(r_h)} \widetilde{u}_h \psi^+)_{j-\frac{1}{2}} = 0, \quad (2.10b)$$

$$\int_{I_j} r_h \eta dx + \int_{I_j} u_h \eta_x dx - (\widehat{u}_h \eta^-)_{j+\frac{1}{2}} + (\widehat{u}_h \eta^+)_{j-\frac{1}{2}} = 0. \quad (2.10c)$$

The numerical fluxes in equations (2.10) are chosen as

$$\widehat{p}_h = p_h^+, \quad \widehat{u}_h = u_h^-, \quad \widehat{B(r_h)} = B(r_h^+), \quad \widetilde{u}_h = u_h^- \quad (2.11)$$

and

$$\widehat{b(r_h)} = \begin{cases} r_h^- & \text{if } u_h^- \geq 0, \\ r_h^+ & \text{if } u_h^- < 0. \end{cases} \quad (2.12)$$

The boundary conditions for the LDG scheme of the HS equation are taken as

$$(u_h)_{\frac{1}{2}}^- = 0, (r_h)_{\frac{1}{2}}^- = 0, (r_h)_{N+\frac{1}{2}}^+ = 0, (p_h)_{N+\frac{1}{2}}^+ = 0. \quad (2.13)$$

The definition of the algorithm is now complete. Notice that we have used the same notation r_h in (2.7b) and in (2.10c) as the schemes as well as the fluxes chosen are identical. The implementation detail of the algorithm can be found in [21].

Remark 2.1. Comparing with the scheme in [21], the main difference of the scheme in this paper is the choice of the numerical flux for $\widehat{b(r_h)}$.

- The numerical flux in [21] is the central flux, i.e.

$$\widehat{b(r_h)} = \frac{B(r_h^+) - B(r_h^-)}{r_h^+ - r_h^-} = \frac{1}{2}(r_h^+ + r_h^-). \quad (2.14)$$

The issue of convergence to its weak solutions of the LDG method in [21] is subtle. It seems that the LDG scheme in [21] without limiters, if converges, should converge to the conservative solution because the numerical solution is energy conservative.

- The numerical flux (2.12) is based on the upwinding principle. The resulting scheme provide additional energy dissipation, thus facilitating convergence towards the dissipative weak solution without any limiters.

Remark 2.2. We remark that the choice for the fluxes is not unique. We can also choose the following numerical fluxes

$$\widehat{r}_h = r_h^-, \widehat{u}_h = u_h^+, \widehat{p}_h = p_h^-, \widehat{B(r_h)} = B(r_h^-), \widetilde{u}_h = u_h^+, \quad (2.15)$$

$$\widehat{b(r_h)} = \begin{cases} r_h^- & \text{if } u_h^+ \geq 0, \\ r_h^+ & \text{if } u_h^+ < 0. \end{cases} \quad (2.16)$$

2.3 Energy stability of the LDG method

In this section, we prove the energy stability of the LDG method for the HS type equations defined in the previous section.

Proposition 2.1. (Energy stability) *The solution to the schemes (2.7) with fluxes (2.8) and (2.10) with fluxes (2.11)–(2.12) satisfies the energy stability*

$$\frac{d}{dt} \int_0^L r_h^2 dx \leq 0. \quad (2.17)$$

Proof. For equation (2.7a), we first take the time derivative and get

$$\int_{I_j} (q_h)_t \rho dx + \int_{I_j} (r_h)_t \rho_x dx - ((\widehat{r_h})_t \rho^-)_{j+\frac{1}{2}} + ((\widehat{r_h})_t \rho^+)_{j-\frac{1}{2}} = 0. \quad (2.18)$$

Since (2.18), (2.7b) and (2.10a)–(2.10c) hold for any test functions in V_h , we can choose

$$\rho = u_h, \quad \vartheta = (r_h)_t, \quad \varphi = -u_h, \quad \psi = -r_h, \quad \eta = p_h.$$

With these choices of test functions and summing up the five equations in (2.18), (2.7b) and (2.10a)–(2.10c), we obtain

$$\begin{aligned} & \int_{I_j} (r_h)_t r_h dx + \int_{I_j} (p_h u_h)_x dx - (\widehat{p_h} u_h^- + \widehat{u_h} p_h^-)_{j+\frac{1}{2}} + (\widehat{p_h} u_h^+ + \widehat{u_h} p_h^+)_{j-\frac{1}{2}} \\ & - \int_{I_j} (B(r_h) u_h)_x dx + (\widehat{B(r_h)} u_h^- + \widehat{b(r_h)} \widetilde{u_h} r_h^-)_{j+\frac{1}{2}} - (\widehat{B(r_h)} u_h^+ + \widehat{b(r_h)} \widetilde{u_h} r_h^+)_{j-\frac{1}{2}} \\ & + \int_{I_j} ((r_h)_t u_h)_x dx - ((\widehat{r_h})_t u_h^- + \widehat{u_h} (r_h^-)_t)_{j+\frac{1}{2}} + ((\widehat{r_h})_t u_h^+ + \widehat{u_h} (r_h^+)_t)_{j-\frac{1}{2}} = 0. \end{aligned}$$

We have

$$\int_{I_j} (r_h)_t r_h dx + \Psi_{j+\frac{1}{2}} - \Psi_{j-\frac{1}{2}} + \Theta_{j-\frac{1}{2}} = 0, \quad (2.19)$$

where the numerical entropy fluxes are given by

$$\begin{aligned} \Psi_{j+\frac{1}{2}} = & \left(p_h^- u_h^- - (\widehat{p_h} u_h^- + \widehat{u_h} p_h^-) \right. \\ & \left. - B(r_h^-) u_h^- + \widehat{B(r_h)} u_h^- + \widehat{b(r_h)} \widetilde{u_h} r_h^- + (r_h^-)_t u_h^- - ((\widehat{r_h})_t u_h^- + \widehat{u_h} (r_h^-)_t) \right)_{j+\frac{1}{2}}, \end{aligned}$$

and the extra term Θ is given by

$$\begin{aligned} \Theta_{j-\frac{1}{2}} = & \left(-[p_h u_h] + \widehat{p_h}[u_h] + \widehat{u_h}[p_h] \right. \\ & \left. + [B(r_h) u_h] - \widehat{b(r_h)} \widetilde{u_h}[r_h] - \widehat{B(r_h)}[u_h] - [(r_h)_t u_h] + (\widehat{r_h})_t [u_h] + \widehat{u_h} [(r_h)_t] \right)_{j-\frac{1}{2}}. \end{aligned}$$

With the definition (2.8) and (2.11) of the numerical fluxes and after some algebraic manipulation, we easily obtain

$$-[p_h u_h] + \widehat{p_h}[u_h] + \widehat{u_h}[p_h] = 0,$$

$$-[(r_h)_t u_h] + \widehat{(r_h)_t}[u_h] + \widehat{u}_h[(r_h)_t] = 0,$$

and

$$\begin{aligned} & [B(r_h)u_h] - \widehat{b(r_h)}\widetilde{u}_h[r_h] - \widehat{B(r_h)}[u_h] & (2.20) \\ &= \frac{1}{2}((r_h^+)^2 - \widehat{B(r_h)})(u_h^+ - u_h^-) + (r_h^+ - r_h^-) \left(\frac{1}{2}(r_h^+ + r_h^-)u_h^- - \widehat{b(r_h)}\widetilde{u}_h \right) \\ &\stackrel{(2.8)}{=} (r_h^+ - r_h^-) \left(\frac{1}{2}(r_h^+ + r_h^-)u_h^- - \widehat{b(r_h)}u_h^- \right) \\ &\stackrel{(2.15)}{=} \begin{cases} \frac{1}{2}(r_h^+ - r_h^-)^2 u_h^- & \text{if } u_h^- \geq 0, \\ -\frac{1}{2}(r_h^+ - r_h^-)^2 u_h^- & \text{if } u_h^- < 0. \end{cases} \\ &\geq 0. \end{aligned}$$

Hence

$$\Theta_{j-\frac{1}{2}} \geq 0. \quad (2.21)$$

Summing up the cell entropy inequalities ((2.19) with (2.21)) and taking care of the boundary conditions (2.13), we obtain

$$\int_I (r_h)_t r_h dx \leq 0. \quad (2.22)$$

This is the desired energy stability (2.17). \square

Remark 2.3. The proof is similar to that in [21]. However, the numerical fluxes (2.15) provide additional energy dissipation in (2.20).

Remark 2.4. For the numerical fluxes (2.15) and (2.16), we can also prove the energy stability (2.17).

3 A new dissipative DG method for the HS equation

In [11], the HS equation is also written in the following form

$$(u_t + uu_x)_x = \frac{1}{2}(u_x)^2 \quad (3.1)$$

with

$$u(0, t) = 0, \quad t \in [0, T] \quad (3.2)$$

and

$$u(x, 0) = u^0(x). \quad (3.3)$$

By introducing

$$r = u_x, \quad (3.4)$$

we may write the equation as

$$r_t + (ur)_x = \frac{1}{2}r^2, \quad r = u_x \quad (3.5)$$

or

$$r_t + ur_x = -\frac{1}{2}r^2, \quad r = u_x. \quad (3.6)$$

In [10], Holden et al. proved that a upwind finite difference method approximating (3.6) converges to the unique dissipative solution of the HS equation (3.6). The dissipative solutions for the HS equation are well studied from a mathematical point of view, we refer the readers to a series of papers [12, 13, 23, 24, 25]. This motivates us to consider a new dissipative DG method which, as we will see later, becomes equivalent to the first order upwind finite difference method in [10] for the piecewise constant P^0 case, thus convergent to the unique dissipative solution of (3.6) in this case. Therefore, this dissipative DG method can be considered as a direct generalization of the method in [10] to high order accuracy.

In the following, we will present this new dissipative DG method and prove its stability. We will also demonstrate that this DG scheme, for the piecewise constant P^0 case, is equivalent to the upwind finite difference scheme in [10].

3.1 The new DG method

The new DG scheme for the equation (3.5) is defined as follows. Find $r_h \in V_h$ such that, for all test functions $\rho \in V_h$,

$$\int_{I_j} (r_h)_t \rho dx - \int_{I_j} u_h r_h \rho_x dx + (u_h \widehat{r}_h \rho^-)_{j+\frac{1}{2}} - (u_h \widehat{r}_h \rho^+)_{j-\frac{1}{2}} = \frac{1}{2} \int_{I_j} r_h^2 \rho dx, \quad (3.7)$$

where

$$u_h = \int_{x_{\frac{1}{2}}}^x r_h(x_1, t) dx_1, \quad (3.8)$$

which is a continuous piecewise polynomial function with degree at most $k + 1$.

The numerical flux \widehat{r}_h in (3.7) is taking as

$$\widehat{r}_h = \begin{cases} r_h^- & \text{if } u_h \geq 0, \\ r_h^+ & \text{if } u_h < 0. \end{cases} \quad (3.9)$$

which is also based on the upwinding principle.

The boundary conditions for the DG scheme of the HS equation are taken as

$$(u_h)_{\frac{1}{2}} = 0, (r_h)_{\frac{1}{2}}^- = 0, (r_h)_{N+\frac{1}{2}}^+ = 0. \quad (3.10)$$

The definition of the algorithm is now complete.

Remark 3.1. The main difference between the DG scheme (3.7) and the LDG scheme (2.7) and (2.10) in Section 2 is the solution u_h .

- u_h in (3.7) is a continuous piecewise polynomial function of degree $k + 1$.
- u_h in (2.7) and (2.10) in Section 2 is a discontinuous piecewise polynomial function of degree k .

The approximations to u_x in both schemes are discontinuous piecewise polynomial functions of degree k .

3.2 Stability of the DG method

Proposition 3.1. (*Stability*) The solution to the scheme (3.7)–(3.9) satisfies the stability

$$\frac{d}{dt} \int_0^L r_h^2 dx \leq 0. \quad (3.11)$$

Proof. Choosing the test function $\rho = r_h$ in (3.7), we obtain

$$\int_{I_j} (r_h)_t r_h dx - \int_{I_j} u_h r_h (r_h)_x dx + (u_h \widehat{r}_h r_h^-)_{j+\frac{1}{2}} - (u_h \widehat{r}_h r_h^+)_{j-\frac{1}{2}} = \frac{1}{2} \int_{I_j} r_h^3 dx.$$

Using integration by parts for the second term in the above equation and noticing the continuity of u_h , we have

$$\begin{aligned} & \int_{I_j} (r_h)_t r_h dx + \frac{1}{2} \int_{I_j} (u_h)_x r_h^2 dx - \frac{1}{2} (u_h(r_h^-)^2)_{j+\frac{1}{2}} + \frac{1}{2} (u_h(r_h^+)^2)_{j-\frac{1}{2}} \\ & + (u_h \widehat{r}_h r_h^-)_{j+\frac{1}{2}} - (u_h \widehat{r}_h r_h^+)_{j-\frac{1}{2}} = \frac{1}{2} \int_{I_j} r_h^3 dx. \end{aligned} \quad (3.12)$$

The second term and the last term in the equation (3.12) will be cancelled because $(u_h)_x = r_h$. Now the equation (3.12) can be written in the following form

$$\int_{I_j} (r_h)_t r_h dx + \Phi_{j+\frac{1}{2}} - \Phi_{j-\frac{1}{2}} + \Theta_{j-\frac{1}{2}} = 0, \quad (3.13)$$

where the numerical entropy fluxes are given by

$$\Phi = u_h \widehat{r}_h r_h^- - \frac{1}{2} (u_h(r_h^-)^2)$$

and the extra term Θ is given by

$$\Theta = u_h \widehat{r}_h r_h^- - u_h \widehat{r}_h r_h^+ - \frac{1}{2} (u_h(r_h^-)^2) + \frac{1}{2} (u_h(r_h^+)^2).$$

With the definition (3.9) of the numerical fluxes and after some algebraic manipulation, we easily obtain

$$\begin{aligned} \Theta &= u_h (r_h^+ - r_h^-) \left(\frac{1}{2} (r_h^+ - r_h^-) - \widehat{r}_h \right) \\ &= \begin{cases} \frac{1}{2} (r_h^+ - r_h^-)^2 u_h & \text{if } u_h \geq 0, \\ -\frac{1}{2} (r_h^+ - r_h^-)^2 u_h & \text{if } u_h < 0. \end{cases} \\ &\geq 0. \end{aligned}$$

Hence

$$\Theta \geq 0. \quad (3.14)$$

Summing up the cell entropy inequalities ((3.13) with (3.14)) and taking care of the boundary conditions (3.10), we obtain

$$\int_I (r_h)_t r_h dx \leq 0. \quad (3.15)$$

This is the desired stability result (3.11). \square

3.3 Convergence of the DG method for the P^0 case

In this section, we discuss the convergence of the DG method in Section 3.1 for the piecewise constant approximation, namely, discontinuous P^0 finite elements.

We denote by v_j , the numerical solution v_h in the cell I_j (it is a constant in each cell). Then from (3.8), we can get

$$(u_h)_{j-\frac{1}{2}} = \sum_{i=1}^{j-1} (v_h)_i h_i \quad (3.16)$$

$$(u_h)_{j+\frac{1}{2}} = \sum_{i=1}^j (v_h)_i h_i, \quad (3.17)$$

$$(u_h)_{j+\frac{1}{2}} - (u_h)_{j-\frac{1}{2}} = (v_h)_j h_j. \quad (3.18)$$

The scheme (3.7)–(3.9) can be rewritten in the explicit form

$$\frac{d}{dt}(v_h)_j h_j + (u_h)_{j+\frac{1}{2}}(v_h)_j - (u_h)_{j-\frac{1}{2}}(v_h)_{j-1} = \frac{1}{2}(v_h)_j^2 h_j, \quad \text{if } u_h > 0, \quad (3.19a)$$

$$\frac{d}{dt}(v_h)_j h_j + (u_h)_{j+\frac{1}{2}}(v_h)_{j+1} - (u_h)_{j-\frac{1}{2}}(v_h)_j = \frac{1}{2}(v_h)_j^2 h_j, \quad \text{if } u_h < 0. \quad (3.19b)$$

In the following, we will prove that the scheme (3.19) can be written in the following form

$$\frac{d}{dt}(v_h)_j + (u_h)_{j-\frac{1}{2}} D_-(v_h)_j = -\frac{1}{2}(v_h)_j^2, \quad \text{if } u_h > 0, \quad (3.20a)$$

$$\frac{d}{dt}(v_h)_j + (u_h)_{j+\frac{1}{2}} D_+(v_h)_j = -\frac{1}{2}(v_h)_j^2, \quad \text{if } u_h < 0 \quad (3.20b)$$

where $D_-(v_h)_j = ((v_h)_j - (v_h)_{j-1})/h_j$ and $D_+(v_h)_j = ((v_h)_{j+1} - (v_h)_j)/h_j$. This is just the semi-discrete finite difference scheme in [10].

Lemma 3.2. *The scheme (3.19) is equivalent to the scheme (3.20).*

Proof. We will prove the Lemma for $u_h > 0$ and $u_h < 0$ respectively.

- $u_h > 0$.

The scheme (3.19a) can be written as

$$\frac{d}{dt}(v_h)_j h_j + (u_h)_{j-\frac{1}{2}}((v_h)_j - (v_h)_{j-1}) + ((u_h)_{j+\frac{1}{2}} - (u_h)_{j-\frac{1}{2}})(v_h)_j = \frac{1}{2}(v_h)_j^2 h_j.$$

Now, using the relation in (3.18), we can obtain

$$\frac{d}{dt}(v_h)_j h_j + (u_h)_{j-\frac{1}{2}}((v_h)_j - (v_h)_{j-1}) + (v_h)_j^2 h_j = \frac{1}{2}(v_h)_j^2 h_j.$$

That is (3.20a)

$$\frac{d}{dt}(v_h)_j + (u_h)_{j-\frac{1}{2}} D_-(v_h)_j = -\frac{1}{2}(v_h)_j^2.$$

- $u_h < 0$.

The scheme (3.19b) can be written as

$$\frac{d}{dt}(v_h)_j h_j + (u_h)_{j+\frac{1}{2}}((v_h)_{j+1} - (v_h)_j) + ((u_h)_{j+\frac{1}{2}} - (u_h)_{j-\frac{1}{2}})(v_h)_j = \frac{1}{2}(v_h)_j^2 h_j.$$

Now, using the relation in (3.18), we can obtain

$$\frac{d}{dt}(v_h)_j h_j + (u_h)_{j+\frac{1}{2}}((v_h)_{j+1} - (v_h)_j) + (v_h)_j^2 h_j = \frac{1}{2}(v_h)_j^2 h_j.$$

That is (3.20b)

$$\frac{d}{dt}(v_h)_j + (u_h)_{j+\frac{1}{2}} D_+(v_h)_j = -\frac{1}{2}(v_h)_j^2.$$

□

Remark 3.2. The equivalence of the schemes (3.19) and (3.20) implies that we can directly get the convergence results for P^0 DG method since the convergence results were proved for (3.20) in [10]. The numerical solution with P^0 polynomial functions will converge to a dissipative solution of HS equation.

Remark 3.3. Because of the equivalency in the P^0 case, the dissipative DG method can be considered as a direct generalization of the method in [10] to high order accuracy. The convergence proof for the DG scheme in P^k with $k \geq 1$ is however more complicated and is left for future work.

4 Numerical results

We will first show the accuracy test results for the upwinding numerical schemes in this paper. We also present one numerical example (Example 4.1 in [21]) here, which contains

the solution with discontinuous derivative, to compare different methods and to show the advantage of the schemes in this paper. The results for other examples in [21] are similar for all the schemes and hence are not shown to save space. Time discretization is by the third order explicit TVD Runge-Kutta method in [18]. This is not the most efficient method for the time discretization to our LDG scheme. However, we will not address the issue of time discretization efficiency in this paper.

Consider the numerical solution of the HS equation

$$u_{xxt} + 2u_x u_{xx} + uu_{xxx} = 0. \quad (4.1)$$

First, we test our method taking the exact solution

$$u(x, t) = 0.01(x - \pi)^2(x + \pi)^2 \sin(x - t) \quad (4.2)$$

for the HS equation with a source term f , which is a given function so that (4.2) is the exact solution. The computational domain is $[-\pi, \pi]$. The L^∞ errors for the numerical solutions of u_h , r_h and the numerical orders of accuracy at time $t = 0.5$ with uniform meshes are contained in Table 4.1. We can see that our schemes in this paper have high order accuracy for the smooth solutions. The observation for the accuracy order is the following:

- The LDG method in Section 2 with the upwinding numerical flux (2.12).

The method with P^k elements gives a uniform $(k+1)$ -th order of accuracy for u_h . For the solution r_h , the accuracy is k -th order for $k \geq 1$.

- The DG method in Section 3 with the upwinding numerical flux (3.9).

The method with P^k elements gives a uniform $(k+2)$ -th order of accuracy for u_h . For the solution r_h , the accuracy is $(k+1)$ -th order for $k \geq 1$. From Table 4.1, we can see that, for the same mesh, the magnitude and order of the error for the DG method are better than those for the LDG method. This is consistent with the different choices of the polynomial degree of u_h for the two methods.

Table 4.1: L^∞ errors and orders of accuracy for the LDG method in Section 2 with the upwinding numerical flux (2.12) and the DG method in Section 3 with the upwinding numerical flux (3.9) for the exact solution (4.2), $t = 0.5$.

		LDG, upwinding flux				DG, upwinding flux			
		u_h		r_h		u_h		r_h	
	N	L^∞ error	order	L^∞ error	order	L^∞ error	order	L^∞ error	order
P^0	10	3.62E-01	–	8.71E-01	–	1.84E-01	–	4.53E-01	–
	20	1.76E-01	1.04	4.86E-01	0.84	9.11E-02	1.02	2.76E-01	0.72
	40	8.72E-02	1.01	2.50E-01	0.96	4.39E-02	1.05	1.45E-01	0.93
	80	4.33E-03	1.01	1.26E-01	0.99	2.16E-02	1.02	7.35E-02	0.98
P^1	10	6.58E-02	–	1.77E-01	–	9.10E-03	–	1.11E-01	–
	20	1.93E-02	1.77	9.17E-02	0.95	1.25E-03	2.86	3.26E-02	1.77
	40	5.15E-03	1.91	4.00E-02	1.20	1.33E-04	3.23	1.00E-02	1.70
	80	1.33E-03	1.96	1.80E-02	1.15	1.60E-05	3.06	2.41E-03	2.06
P^2	10	8.03E-03	–	4.86E-02	–	7.97E-04	–	1.43E-02	–
	20	1.18E-03	2.76	1.50E-02	1.70	4.41E-05	4.18	2.03E-03	2.82
	40	1.71E-04	2.79	3.78E-03	1.99	2.53E-06	4.13	2.42E-04	3.06
	80	2.03E-05	3.07	1.02E-03	1.88	1.84E-07	3.78	3.27E-05	2.89
P^3	10	6.19E-04	–	1.09E-02	–	1.94E-04	–	5.80E-03	–
	20	5.26E-05	3.56	1.25E-03	3.13	2.81E-06	6.11	1.87E-03	4.95
	40	3.44E-06	3.93	1.51E-04	3.04	5.53E-08	5.67	6.93E-06	4.75
	80	2.55E-07	3.76	1.94E-05	2.96	2.02E-09	4.77	3.42E-07	4.34

Next, we consider the initial condition

$$u(x, 0) = \begin{cases} 0, & \text{if } x \leq 0, \\ x, & \text{if } 0 < x < 1, \\ 1, & \text{if } 1 \leq x. \end{cases} \quad (4.3)$$

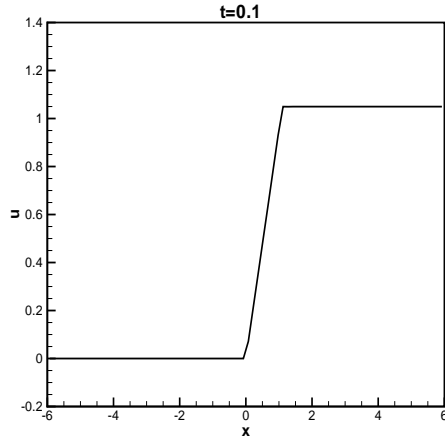
The exact solution of the HS equation (4.1) with the initial condition (4.3) is

$$u(x, t) = \begin{cases} 0, & \text{if } x \leq 0, \\ \frac{x}{(0.5t+1)}, & \text{if } 0 < x < (0.5t+1)^2, \\ (0.5t+1), & \text{if } x \geq (0.5t+1)^2. \end{cases} \quad (4.4)$$

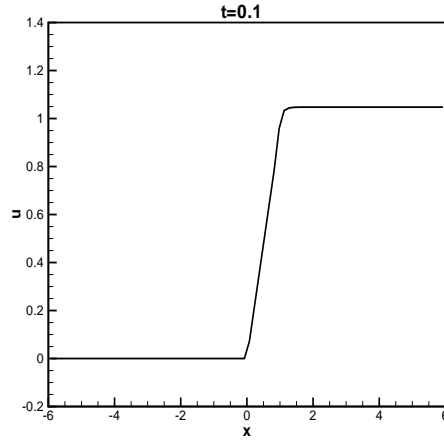
The computational domain is $[-6, 6]$. Even though the solution u is continuous, the lack of smoothness of u_x will introduce high-frequency oscillation into the calculation of the residual. To compare the performance of the different methods, we use the following methods in the computations by P^2 elements with $N = 80$ cells for the solution u and r (i.e. u_x).

- (a) The LDG method in [21] with the central numerical flux (2.14).
- (b) The LDG method in [21] with the central numerical flux (2.14) and the total variation bounded in the means (TVBM) limiter in [4] to control the oscillation of r_h .
- (c) The LDG method in Section 2 with the upwinding numerical flux (2.12).
- (d) The DG method in Section 3 with the upwinding numerical flux (3.9).

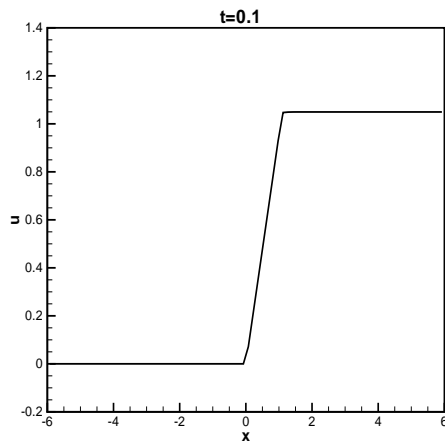
We show the numerical solutions u_h in Figures 4.1–4.2 and r_h in Figures 4.3–4.4. We can see that the central scheme (a) without limiter generates spurious oscillation in r_h approximating u_x near its discontinuity, especially at the later time $t = 0.5$. The TVBM limiter (b) removes these oscillations in r_h , at the price of smearing the derivative discontinuity and smoothing out the solution u as well. The numerical solutions based on the upwinding schemes (c)–(d) have much sharper fronts than those with the TVBM limiter, with just slight, localized over and under-shoots near the fronts. In Figure 4.5, the energy $\int_0^L r_h^2 dx$ as a function of time for the numerical solutions is shown. The solution of r for scheme (a) is oscillatory without the limiter, but the energy is still conserved. When the limiter is used, the energy is decaying a lot. The upwinding schemes (c)–(d) provide additional energy dissipation (but not too much), thus facilitating convergence towards the weak solution without any limiters.



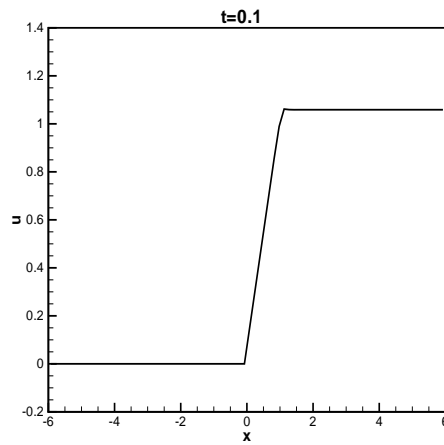
(a) LDG, central flux



(b) LDG, limiter



(c) LDG, upwinding flux

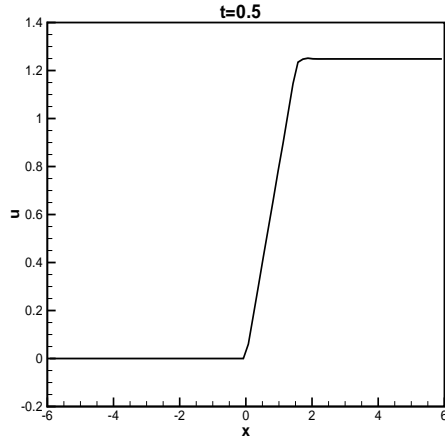


(d) DG, upwinding flux

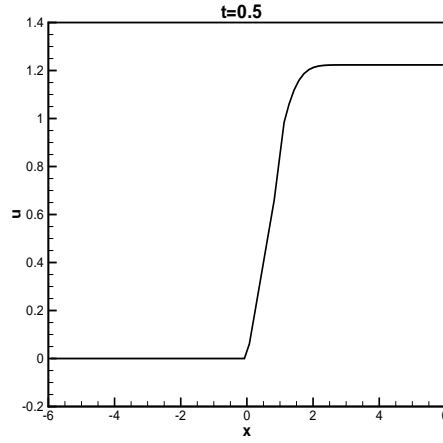
Figure 4.1: Solution u for the HS equation (4.1) the initial condition (4.3) for different schemes at $t = 0.1$.

5 Conclusion

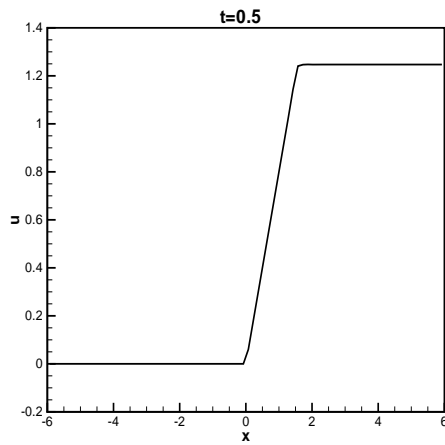
We have developed dissipative LDG and DG methods to solve the HS type equations. Energy stability is proved for general solutions for both schemes. Convergence of the DG scheme for the P^0 case is proved by showing its equivalency with the upwind scheme in [10]. An important issue not addressed in this paper is convergence proof for high order DG methods. From the stability and approximation results, we can derive L^2 a priori



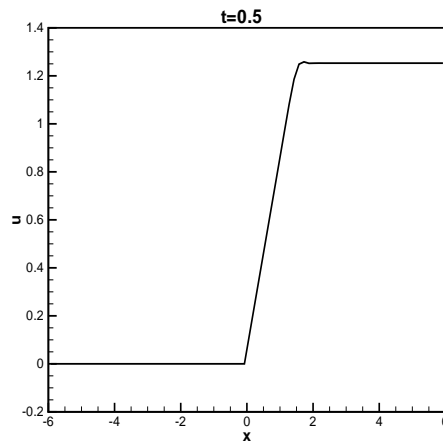
(a) LDG, central flux



(b) LDG, limiter



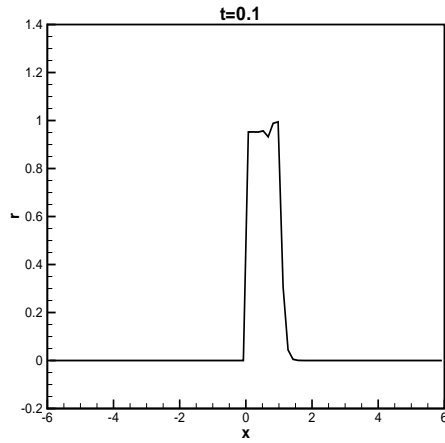
(c) LDG, upwinding flux



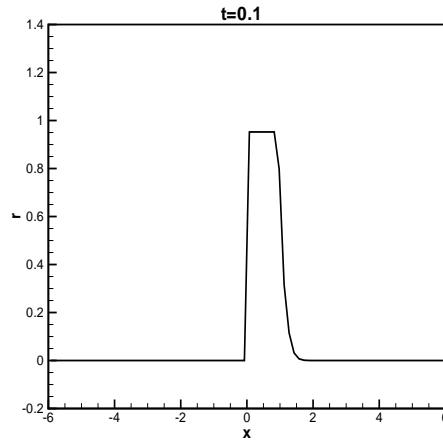
(d) DG, upwinding flux

Figure 4.2: Solution u for the HS equation (4.1) the initial condition (4.3) for different schemes at $t = 0.5$.

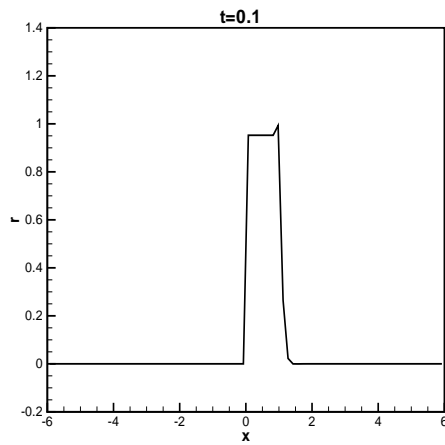
error estimates of the high order LDG method for the Camassa-Holm equation [20]. However the proof of the high order DG method for the HS equation is not completely straightforward. Such proof is left for future work.



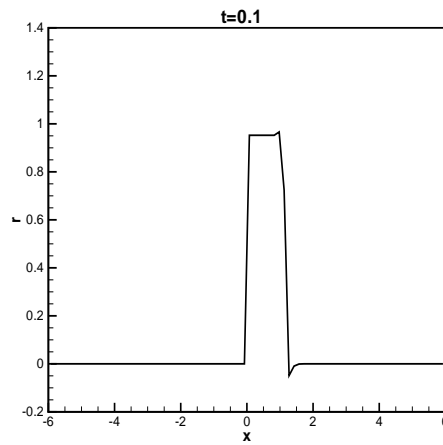
(a) LDG, central flux



(b) LDG, limiter



(c) LDG, upwinding flux

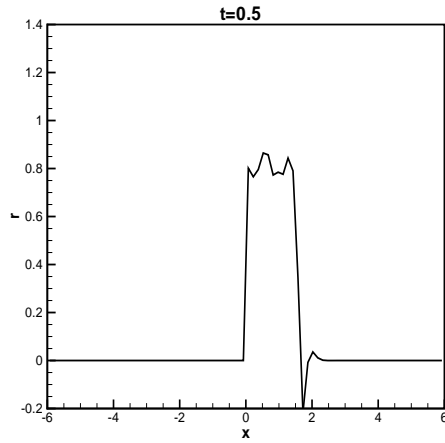


(d) DG, upwinding flux

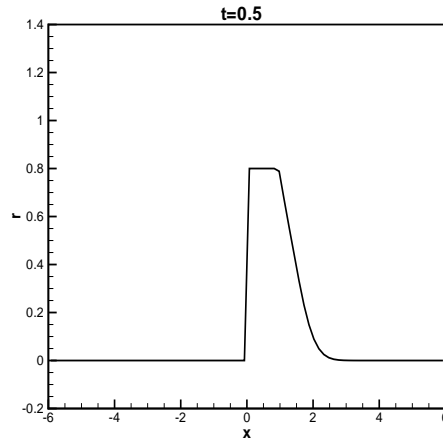
Figure 4.3: Solution r (i.e. u_x) for the HS equation (4.1) the initial condition (4.3) for different schemes at $t = 0.1$.

References

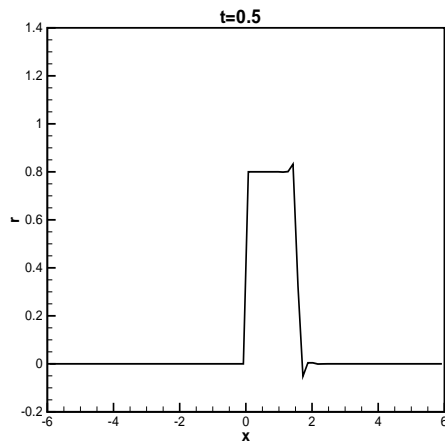
- [1] F. Bassi and S. Rebay. A high-order accurate discontinuous finite element method for the numerical solution of the compressible Navier-Stokes equations. *J. Comput. Phys.*, 131:267–279, 1997.
- [2] B. Cockburn, S. Hou, and C.-W. Shu. The Runge-Kutta local projection discontinuous Galerkin finite element method for conservation laws IV: the multidimensional



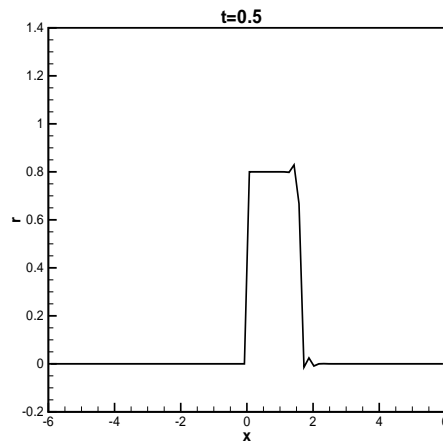
(a) LDG, central flux



(b) LDG, limiter



(c) LDG, upwinding flux



(d) DG, upwinding flux

Figure 4.4: Solution r (i.e. u_x) for the HS equation (4.1) the initial condition (4.3) for different schemes at $t = 0.5$.

case. *Math. Comp.*, 54:545–581, 1990.

[3] B. Cockburn, S.-Y. Lin, and C.-W. Shu. TVB Runge-Kutta local projection discontinuous Galerkin finite element method for conservation laws III: one dimensional systems. *J. Comput. Phys.*, 84:90–113, 1989.

[4] B. Cockburn and C.-W. Shu. TVB Runge-Kutta local projection discontinuous Galerkin finite element method for conservation laws II: general framework. *Math.*

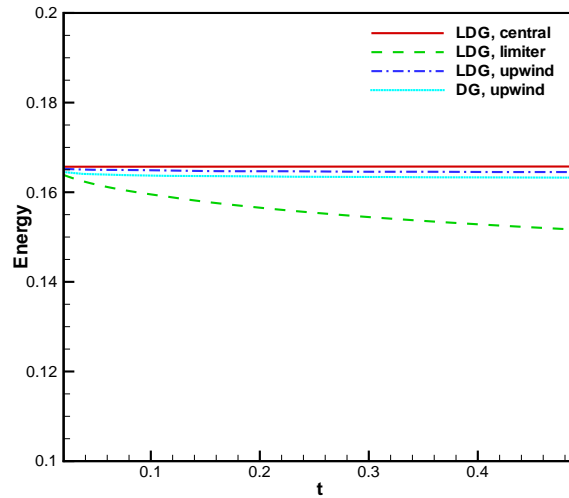


Figure 4.5: Energy of the different schemes for the HS equation (4.1) the initial condition (4.3).

Comp., 52:411–435, 1989.

- [5] B. Cockburn and C.-W. Shu. The local discontinuous Galerkin method for time-dependent convection-diffusion systems. *SIAM J. Numer. Anal.*, 35:2440–2463, 1998.
- [6] B. Cockburn and C.-W. Shu. The Runge-Kutta discontinuous Galerkin method for conservation laws V: multidimensional systems. *J. Comput. Phys.*, 141:199–224, 1998.
- [7] B. Cockburn and C.-W. Shu. Foreword for the special issue on discontinuous Galerkin method. *J. Sci. Comput.*, 22-23:1–3, 2005.
- [8] C. Dawson. Foreword for the special issue on discontinuous Galerkin method. *Comput. Methods Appl. Mech. Engin.*, 195:3183, 2006.
- [9] J. Hesthaven and T. Warburton. *Nodal discontinuous Galerkin methods. Algorithms, analysis, and applications*. Springer, 2008.
- [10] H. Holden, K. Karlsen, and N. Risebro. Convergent difference schemes for the Hunter–Saxton equation. *Math. Comp.*, 76:699–744, 2007.

- [11] J. Hunter and R. Saxton. Dynamics of director fields. *SIAM J. Appl. Math.*, 51:1498–1521, 1991.
- [12] J. Hunter and Y. Zheng. On a completely integrable nonlinear hyperbolic variational equation. *Physica D*, 79:361–386, 1994.
- [13] J. Hunter and Y. Zheng. On a nonlinear hyperbolic variational equation: I. Global existence of weak solutions. *Arch. Rat. Mech. Anal.*, 129:305–353, 1995.
- [14] B. Li. *Discontinuous finite elements in fluid dynamics and heat transfer*. Springer-Verlag London, 2006.
- [15] W. Reed and T. Hill. Triangular mesh methods for the neutron transport equation. La-ur-73-479, Los Alamos Scientific Laboratory, 1973.
- [16] B. Rivière. *Discontinuous Galerkin methods for solving elliptic and parabolic equations. Theory and implementation*. SIAM, 2008.
- [17] C.-W. Shu, Discontinuous Galerkin methods: general approach and stability, *Numerical Solutions of Partial Differential Equations*, S. Bertoluzza, S. Falletta, G. Russo and C.-W. Shu, *Advanced Courses in Mathematics CRM Barcelona*, Pages 149-201. Birkhäuser, Basel, 2009.
- [18] C.-W. Shu and S. Osher. Efficient implementation of essentially non-oscillatory shock-capturing schemes. *J. Comput. Phys.*, 77:439–471, 1988.
- [19] Y. Xu and C.-W. Shu. Local discontinuous Galerkin methods for two classes of two dimensional nonlinear wave equations. *Physica D*, 208:21–58, 2005.
- [20] Y. Xu and C.-W. Shu. A local discontinuous Galerkin method for the Camassa-Holm equation. *SIAM J. Numer. Anal.*, 46:1998–2021, 2008.
- [21] Y. Xu and C.-W. Shu. Local discontinuous Galerkin method for the Hunter-Saxton equation and its zero-viscosity and zero-dispersion limit. *SIAM J. Sci. Comput.*, 31:1249–1268, 2008.

- [22] J. Yan and C.-W. Shu. A local discontinuous Galerkin method for KdV type equations. *SIAM J. Numer. Anal.*, 40:769–791, 2002.
- [23] P. Zhang and Y. Zheng. On oscillations of an asymptotic equation of a nonlinear variational wave equation. *Asymptot. Anal.*, 18:307–327, 1998.
- [24] P. Zhang and Y. Zheng. On the existence and uniqueness of solutions to an asymptotic equation of a variational wave equation. *Acta Math. Sin. (Engl. Ser.)*, 15:115–130, 1999.
- [25] P. Zhang and Y. Zheng. Existence and uniqueness of solutions of an asymptotic equation arising from a variational wave equation with general data. *Arch. Ration. Mech. Anal.*, 155:49–83, 2000.